Evidence for target outer-shell excitation mediated by electron correlation in single-electron-capture collisions of slow He^{2+} ions with Ar atoms

Z. Y. Song [1,2,*] X. C. Wang [2,3] Z. W. Li,[4] K. L. Han,[4] and D. Fischer[5,†]

[1]*Institute of Modern Physics, Chinese Academy of Sciences, Nanchang Road 509, 730000 Lanzhou, China*
[2]*Max-Planck Institute for Nuclear Physics, Saupfercheckweg 1, D-69117 Heidelberg, Germany*
[3]*School of Physical Science and Technology, ShanghaiTech University, 201210 Shanghai, China*
[4]*Dalian Institute of Chemical Physics, Chinese Academy of Science, 116023 Dalian, China*
[5]*Physics Department and LAMOR, Missouri University of Science & Technology, Rolla, Missouri 65409, USA*

(Received 17 March 2020; accepted 12 October 2020; published 28 October 2020)

We have performed kinematically complete experiments on single-electron capture in slow He^{2+}-Ar collisions. Besides the pure capture to the $He^{+}(n = 2)$ level, capture into the deep $He^{+}(n = 1)$ state with simultaneous excitation of another target electron is also observed. In contrast to the pure capture, the total cross section for this two-electron transition decreases with increasing collision energy, and its angular-differential cross section exhibits a much slighter slope. We take these observations as evidence for electron capture mediated by electron-electron interactions.

DOI: 10.1103/PhysRevA.102.042820

I. INTRODUCTION

The process of correlated two-electron transition generally exists in the field of atomic physics. Autoexcitation and Auger transition occurring in separated atoms, for example, are such physical processes. In slow ion-atom and ion-surface collisions, the inner-shell vacancy production of the projectile was interpreted through the inverse autoexcitation [1] and the internal dielectronic excitation mechanisms [2], respectively. Another example of the correlated two-electron process, in ion-atom collisions, is the correlated double-electron capture [3], which is different from the sequential double capture. All of these processes, in separated atoms or collisions, are mediated by electron-electron interactions (in the following referred to as e-e interaction), which may lead to pronounced electron correlation effects.

The transfer target excitation (TTE) in ion-atom collisions, that is, the process in which the projectile captures a target electron with excitation of another one is also a potential candidate for exploring the correlated two-electron transition since it contains only two collision fragments and no continuum electrons in the final states. In the collisions of protons with He atoms, Hasan *et al.* [4] observed the TTE reaction with collision energies from 25 to 75 keV and found an enhancement for the ratio of TTE to pure single-electron capture (PSEC) and double to single excitation cross section around scattering angle $\theta_P \approx 0.5$ mrad. Theoretical works [5–7] indicated that this enhancement is not related to the correlated two-electron transitions. By increasing the collision energy to 240–2500 keV, SchOoffler and co-workers further investigated the TTE reaction for this collision system [8] and also found a peak structure around $\theta_P \approx 0.5$ mrad for the ratio of TTE and PSEC. They attributed it to the further momentum exchange between the projectile and another target electron in the second interaction of an independent two-step process. In contrast to the strong electron correlation in double capture, Schulz *et al.* [9] pointed out that the e-e interaction is unimportant in the final state of TTE for the p+He collisions. In slow collisions of the highly charged ions with He atoms, Andersson *et al.* [10] found an enhancement (a depleting) of the cross section for one- (two-) electron removal from the target. By extending the molecular classical overbarrier model [11], Cederquist [12] explained the experiments with a three-step mechanism, in which the loosely bound one of the two consecutively captured electrons is recaptured at a critical internuclear distance by the target to its excited state (TTE) because of the interaction of the double-capture quasimolecular channel and the TTE channel. Target excitation through this re-capture mechanism was also observed following multiple-electron capture in collisions of $^{15}N^{7+}$ ions with Ar atoms [13]. A more complicated mechanism called postcollision interaction or autotransfer to Rydberg state was also proposed by Roncin *et al.* [14,15] to interpret the TTE reaction in low-energy collisions of highly charged ions with atoms. Fritsch calculated the cross section of TTE in slow C^{6+} + He collisions and found that it was larger than that for single-electron excitation [16], which is an indication of the correlated two-electron transition since the product of independent transfer and excitation probabilities would always result in a smaller probability than either.

*songzhy@impcas.ac.cn
†fischerda@mst.edu

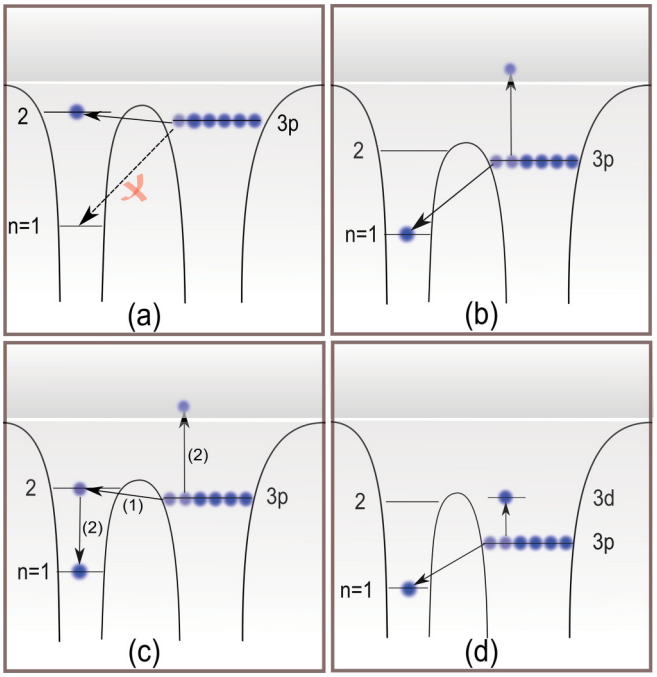

FIG. 1. Schematic of the pure single-electron capture (PSEC) (a), transfer ionization (b), two-step transfer ionization (c), and transfer target excitation (TTE) processes (d).

In the present work, we show evidence for target excitation mediated by the e-e interaction in single-electron capture collisions of He^{2+} ions with Ar atoms. Since the e-e interaction is relatively weak (0.1 a.u. or less) [17,18] as compared to nuclear-electron coupling, the collision energy is selected as 11.3 and 21.8 keV. When the He^{2+} ion approaches the target atom, the potential barrier between the two nuclei gradually decreases. At a certain distance, it will quasiresonantly capture a valence electron to its $n = 2$ orbital. For the low-energy collisions in our experiments, it is impossible to capture the valence electron into the $n = 1$ orbital [Fig. 1(a)]. However, our work puts forward that the e-e interaction enables this capture channel to occur at a relatively small internuclear distance and another valence electron will be excited due to the recoil force [Fig. 1(d)]. At moderate distances, the occurrence of transfer ionization is possible in much the same way as the TTE process [Fig. 1(b)]. Other correlated two-electron transitions such as the two-step process as shown in Fig. 1(c) could also produce the Ar^{2+} ions. Atomic units are used throughout unless indicated otherwise.

II. EXPERIMENTAL APPARATUS

The experiments were performed by using a reaction microscope in Max-Planck Institute for Nuclear Physics in Heidelberg. The details of the reaction microscope and the beamline have been described elsewhere [19], and then some improvements have been made [20,21]. In brief, He^{2+} ions were extracted from a Penning Source, as shown in Fig. 2, then analyzed by a switching magnet. The extraction voltage was 5.7 and 10.9 kV, respectively. After collimated and cleaned by a pair of slits, the ion beam was directed through an annular position-sensitive detector (PSD), which is for detecting the recoil ions, then was intersected with a supersonic cooled Ar target jet in the center of the reaction microscope. After collisions, the scattered ions passed through another annular PSD, and then the He^+ ions were selected by a cylindrical plate spectrometer and detected by a rounded PSD. The recoil ions were accelerated and extracted by a homogeneous electric field (here $\frac{60}{11}$ V cm^{-1}) oriented opposite to the beam direction, then entered into a field-free drift region that is satisfying the time-focusing operation condition, and finally were measured by the recoil-ion PSD. In experiments, we recorded both the time of flight and position of the recoil argon ions in coincidence with the scattered He^+ projectiles.

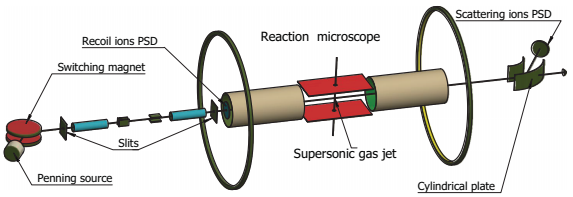

FIG. 2. Schematic diagram for the experimental setup.

For an inelastic collision involving two reaction products, such as the PSEC or TTE process, the recoil ion momentum depends only on the reaction Q value, i.e., the difference of binding energies of all electrons in the final and the initial states. In the case of small scattering angles and small changes in projectile energy, the longitudinal momentum for the recoil ion is given by $P_{\parallel} = \frac{Q}{v_P} - \frac{v_P}{2}$, where v_P is the projectile velocity. Hence the populated electronic states could be accessed via the precise measurements of the recoil-ion longitudinal momentum, which is determined by the time of flight.

III. RESULTS AND DISCUSSION

Figures 3(a) and 3(b) show the Q-value spectra of the recoil Ar^+ ions measured in coincidence with the scattered He^+ ions at collision energies of 21.8 and 11.3 keV, respectively. As shown, the Q-value spectrum consists of two peaks. As discussed in Refs. [22–24], the stronger peak on the right corresponds to the PSEC reaction, i.e., a valence electron of the Ar atom is captured to the $n = 2$ orbital of the He^+ ion,

$$He^{2+} + Ar \rightarrow He^+(n = 2) + Ar^+(3p^5). \quad (1)$$

At the collision energy of 21.8 keV, as shown in Fig. 3(a), the reaction window seems to spread to populate the $n = 3$ orbital. This is in agreement with the prediction of the molecular classical overbarrier model [11] that the reaction window will expand with the increase of the collision energy, which has been confirmed in other collision systems [21,25]. Figure 3 also shows that the relative intensity of the PSEC process increases with increasing collision energy, which could be interpreted by taking the endothermicity of this process ($\sim$2.15 eV) into account. It should be noted that no electron capture to the $n = 1$ orbital of He^+ ($Q = -38.66$ eV) was observed in any of the measurements. The collision energy for opening this capture channel is roughly estimated to be 280 keV by using the uncertainty relation $Q\lambda/v_P \geqslant 1/2$ (setting λ, the effective range of interatomic forces, to 1.0).

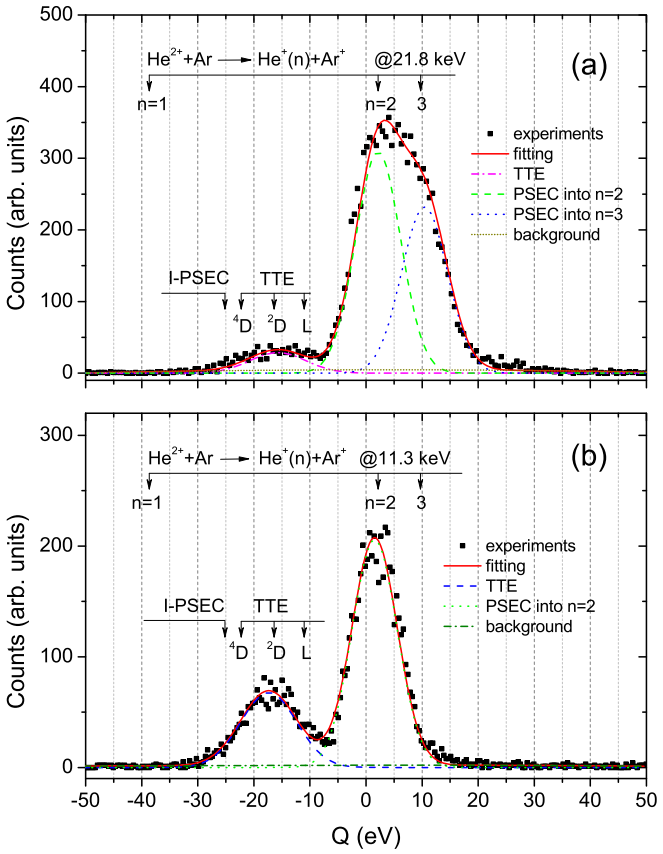

FIG. 3. Q-value spectrum for PSEC and TTE processes in collisions of He^{2+} ions with Ar target at (a) 21.8 and (b) 11.3 keV, respectively. The right peak represents the PSEC; the left peak represents the TTE process. The inner-shell pure single-electron capture (I-PSEC) represents the capture of a $3s$ electron. The atomic terms ^4D, ^2D, and L represent another $3p$ electron excitation into the first state, the state of $Ar^+(3s^23p^4[^1D]3d)[^2D]$, and the energy limit, respectively.

Figure 3 also shows a lower intensity peak on the left side of the Q-value spectra. For this collision system, Panov *et al.* [26] predicted in 1980 that, when the collision energy is less than 15 keV, only the TTE process can occur. However, both the PSEC and TTE processes have been observed in our experiments, but the TTE process becomes stronger as the collision energy decreases. The TTE process can be expressed as

$$He^{2+} + Ar \rightarrow He^+(n = 1) + Ar^+(3s^23p^4nl). \qquad (2)$$

The electron configuration $Ar^+(3s^23p^4nl)$ includes a large number of states, which are not resolved in the measurements. The first excitation state ^4D and the ionization limit L for the $Ar(3s^23p^5)$ configuration are labeled in Fig. 3. The center of the peak corresponds to the $Ar^+(3s^23p^4[^1D]3d)[^2D]$ state. Note that the total spin is zero for the four residue electrons in the $3p$ shell, so it means one of a pair of electrons with opposite spins in the initial state is captured to the $n = 1$ orbital of He^+ and the other one is excited to the $3d$ shell of Ar^+. The configuration consisting of four $3p$ electrons with a total spin of zero and one $3d$ electron contains 11

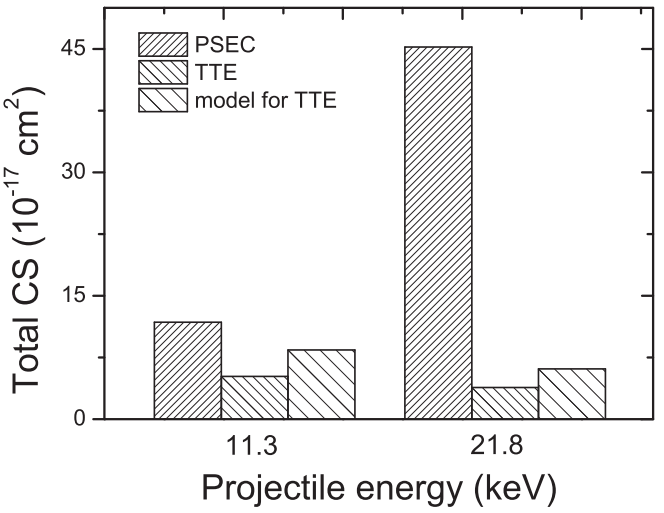

FIG. 4. Measured total cross sections for the PSEC and the TTE processes at two collision energies. The Stolterfoht's model results [1] are also plotted for the TTE.

energy levels. The inner-shell PSEC process, $He^{2+} + Ar \rightarrow He^+(n = 1) + Ar^+(3s3p^6)$, is also labeled in Fig. 3.

Figure 4 shows the total cross sections for the PSEC and the TTE processes, which were obtained by normalizing the integrated counts of the right and the left peaks in the Q-value spectrum, respectively, to the total cross section for the He^+ production from Refs. [27–29]. Since the incident ions are $^3He^{2+}$ rather than $^4He^{2+}$ in Refs. [27,28], we used the data with the same velocity rather than the same kinetic energy as our experiments to normalize our results. There are about 5% discrepancies between the total cross sections obtained from the data in [27,28] and those in [29]. As shown in Fig. 4, the PSEC cross section quickly increases from about 12 to 45×10^{-17} cm^2 as the collision energy increases from 11.3 to 21.8 keV. However, the cross section for the TTE process decreases slightly. This indicates that the mechanism is different for these two processes. The nuclear motion plays a significant role in the PSEC process; nevertheless, not in the TTE.

In slow ion-atom collisions, the quasimolecular framework has been proven to be very powerful in dealing with the inner-shell excitation, ionization, and vacancy transfer processes [30–33]. For this asymmetric He^{2+} and Ar system, a unique feature is the matching of the K-shell level of He with that of the M shell of Ar; thus the adiabatic diagram of orbital energies (Fig. 5), which is calculated by using the GAMESS packages [34], can serve as the starting point for discussing the experimental results. As shown in Fig. 5, the energy for the 5σ molecular orbital (MO), which is correlated with the $3p$ shell of Ar, decreases swiftly with the decrease of the internuclear distance. At about 2.0 a.u., a resonance condition is created and makes an electron in the 5σ MO transit to the $1s$ level of He^+ and another one with opposite spin transit to, for example, the $3d$ excited level of Ar. The orbital selection rules are that the sum $\sum \Delta m_l$ is unchanged and that the parity of the *product* of the MO's is the same [17]. Although limited by these rules, there are a large number of such transitions due to a large number of high-lying excited states of Ar. It should be

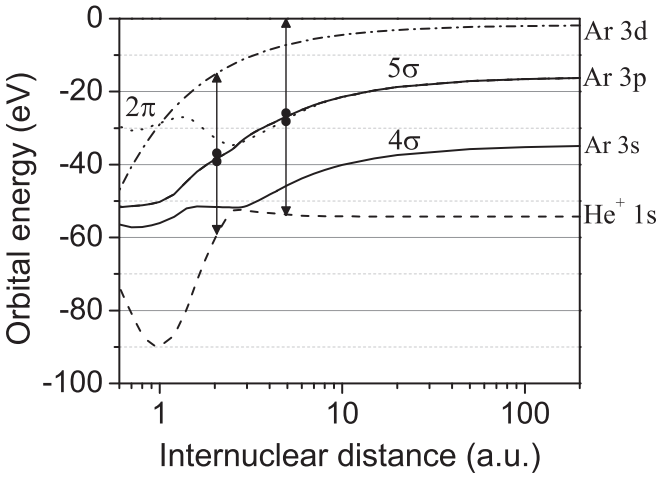

FIG. 5. Computed MO energies for the He^{2+}-Ar system as a function of internuclear distance R. The σ orbitals (or π orbitals) are indicated by solid (dotted) lines; the atomic character of each MO is shown to the right. The unoccupied orbital of $He^{+}(1s)$ is plotted by dashed lines. The excited level of Ar($3d$) is calculated using the Coulomb formula $E(3d) = -1.7–27.2/R$. Note that the resonance condition is created near $R = 2.0$ a.u., allowing the TTE process to occur.

noted that this correlated two-electron transition occurs only as the projectile velocity v_P is less than the electron velocity.

In slow $Ar^+ + SiH_4$ collisions, Stolterfoht proposed a correlated two-electron mechanism called inverse autoexcitation to interpret the Ar L-vacancy production and gave an empirical formula to estimate the probability for such a dielectronic process [1],

$$P(R_c) = 2\pi \frac{N_f |V_{if}(R_c)|^2 R_c^2}{0.7 v_P}, \tag{3}$$

where R_c is the critical distance between the two nuclei (2.0 a.u. here), N_f is the number of final states (11 here), and $V_{if}(R) \approx 0.2 \exp(-\alpha R)$ is the e-e coupling matrix element. Here, $\alpha = 0.86(\sqrt{2B_i} + \sqrt{2B_f})/2$ with B_i and B_f being the binding energies of the transferred electron in the initial and final states, respectively. The Coulomb "force" $F = 1/R^2$ is used here for simplicity [35]. Based on Eq. (3), we evaluated the total cross section of the TTE process by assuming a constant probability inside the critical distance, i.e., $\sigma_{\mathrm{TTE}} = \pi R_c^2 P(R_c)$. Although the calculated results overestimate the experiments by a factor of ~1.5, as shown in Fig. 4, they basically describe the decreasing behavior of the TTE as increasing the collision energy.

Similar to the correlated TTE process, another correlated two-electron process called transfer ionization (TI), in which one $3p$ electron of Ar is ionized simultaneously due to the "huge" potential energy liberated from the capture of another electron to the $n = 1$ orbital of He^+, may occur at an internuclear distance of about 4.9 a.u., as shown in Fig. 5 and Fig. 1(b). Because of the similarity between the TI and TTE, the cross section of Ar^{2+} ions produced by the TI process should increase also with decreasing collision energy. Figure 6 shows the longitudinal momentum spectra of the recoil Ar^{2+} ions, which were measured in coincidence with the He^+ ions.

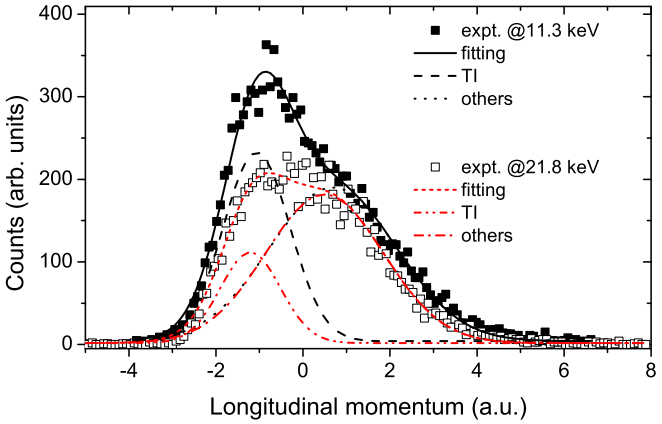

FIG. 6. Longitudinal momenta for recoil Ar^{2+} ions measured in coincidence with He^+ ions for 11.3 (solid square) and 21.8 (hollow square) keV collisions, respectively. The fitting curves are just to guide the eyes.

In addition to the TI, several other processes would contribute to the production of the Ar^{2+} ions. For the collision velocities explored here, the longitudinal momenta less than zero approximately correspond to the TI, while those greater than zero correspond to autoionization double electron capture and other processes, such as the one shown in Fig. 1(c). All these processes were not resolved in the present measurements. However, as shown in Fig. 6, the segment representing the TI process behaves in much the same way as the TTE process as the collision velocity changes.

In single-electron capture collisions of He^{2+} ions with Ar atoms [22,27], more production of the recoil Ar^{2+} than Ar^+ ions had been found as the incident ion energy is dropped from about 30 to 5 keV, while for the Ne, Kr, and Xe targets the most recoil ions are always the single charged ions. The authors attributed these findings to the endothermicity of Eq. (1) and the favored crossing radius for Ar [22,27]. The same results were observed in our experiments, as shown in Table I. In view of the similar behavior of the TI and TTE with the change of the collision velocity, we assume that the increase in the relative intensity of Ar^{2+} ions comes only from the TI reaction and the intensity ratio of TI to TTE is independent of the velocity. Thus the fractions of the Ar^{2+} ions produced due

TABLE I. Relative intensity I_{rel} for recoil Ar ions and corresponding total cross section (TCS) measured in coincidence with the scattered He^+ ions. Estimation of the production for the Ar^{2+} ions by the TI and other mechanisms is listed in the last two rows. The units for the TCS are 10^{-17} cm^2.

	11.3 keV		21.8 keV	
Recoil ion	I_{rel} (%)	TCS	I_{rel} (%)	TCS
Ar^+ (PSEC)	25	11.8	47	45.2
Ar^+ (TTE)	11	5.2	4	3.8
Ar^{2+}	60	28.3	40	38.5
Ar^{3+}	4	1.9	9	8.7
Ar^{2+}(TI)	31	14.6	11	10.6
Ar^{2+}(others)	29	13.6	29	27.9

to the TI and other processes could be resolved (listed in the last two rows of Table I). The fact that more than 50% of the Ar^{2+} ions are produced by the TI process in low-energy collisions means that the ejected electron spectrum would have a significant fraction of continuous distribution, on which linear electron spectra from autoionization double electron capture and other processes are superposed.

Our experimental results could not be explained by other theoretical models, such as the two step [8], the recapture following consecutive two-electron capture [12,13], and the postcollision interaction mechanism [14,15]. According to the two-step mechanism [8], the cross section of the TTE or TI should increase with increasing collision energy since the independent electron capture and target excitation are monotonic increasing functions of the collision energy. In the three-step model [12,13], two electrons will be consecutively captured to corresponding resonant states; then the first captured electron (loosely bound in the $n = 2$ orbital) will be recaptured by the target ion to an excited state with a further decrease of the internuclear distance. Except for the positive correlation between the electron capture cross section and the collision energy, the pure electron capture to the deeper bound state (here $n = 1$) is not observed in our experiments. Therefore, this mechanism can be excluded. For the postcollision interaction or autotransfer to the Rydberg state model [14,15], the TTE originates from the captures of two electrons to a doubly excited state of He; then one of the two electrons decays to the *1s* orbital, while the other one autotransfers first to the Rydberg states and then finally is recaptured by the Ar^{2+} ions to an excited state. However, the significant energy difference between the captured states and the $n = 1$ of He will lead directly to an autoionization of the second electron rather than its transition to the high Rydberg states. This complicated mechanism is somewhat similar to the autoionization double capture and also involves the e-e interaction.

Another piece of evidence is related to the discrepancies between the angular-differential cross sections for the SPEC and the TTE processes. As shown in Fig. 7, the angular distribution for the TTE process exhibits a much slighter slope after it reaches the maximum, while that for the PSEC has a sharp decrease. Roughly, the segment for scattering angles below 1.0 mrad is primarily due to the momentum exchange between the projectile and the electron, while those in larger angles are because of the nucleus-nucleus scattering. As mentioned above, the PSEC process is caused by the interaction between the incident ion and the target electron, so its angular distribution will have a sharp peak in the small-angle part. On the contrary, the TTE proceeds through the correlated two-electron process governed by the e-e interaction, so there is no sharp peak in the small-angle part. In other words, the angle distribution of the TTE primarily originates from the nucleus-nucleus scattering and the e-e interaction is independent of the scattering angle explored in the present experiments.

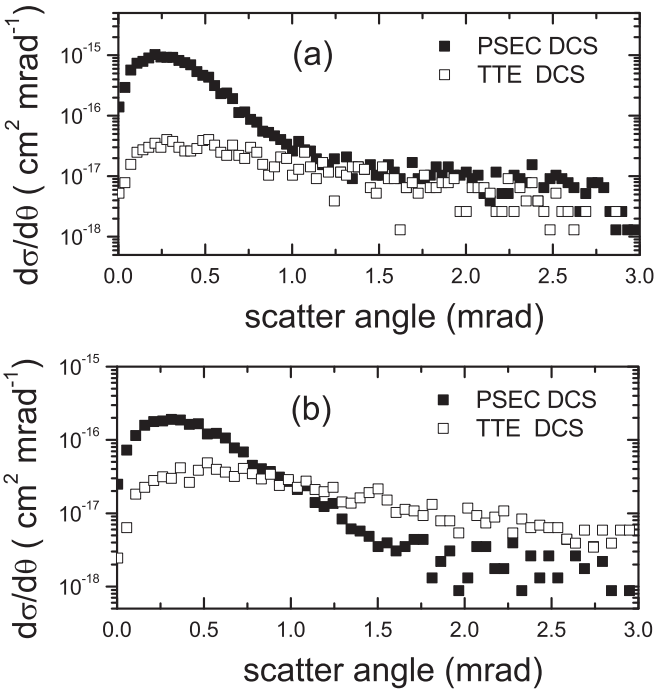

FIG. 7. Angular-differential cross sections for the PSEC and TTE processes as functions of the laboratory scattering angles for (a) 21.8 and (b) 11.3 keV He^{2+}-Ar collisions.

IV. CONCLUSIONS

In conclusion, we have performed kinematically complete experiments on single-electron capture in slow collisions of He^{2+} ions with Ar atoms and observed two reactions, namely, the PSEC and the TTE. In contrast to the PSEC process, the total cross section of the TTE decreases slightly with the increase of the collision energy. Moreover, by using the calculated critical internuclear distance, Stolterfoht's model that accounts for the correlated two-electron transition probability can approximately describe the behavior of the TTE cross section. Also, a similar correlated two-electron process called TI behaves in much the same way as the TTE as the collision energy changes. The much smoother distribution for the angular-differential cross section of the TTE, as compared to the steeply decreasing for the PSEC, gives further evidence that the TTE is caused by e-e interaction. In short, our work unveils strong evidence that the TTE reaction in slow collisions of He^{2+} ions with Ar atoms is a correlated two-electron transition process.

ACKNOWLEDGMENTS

This work is partly supported by the National Key R&D Program of China under Grant No. 2017YFA0402300 and the National Natural Science Foundation of China through Grant No. 11675279. This work is also supported by Chinese Academy of Sciences-Max-Planck Society Joint Doctoral Promotion Program. Z.Y.S. thanks Dr. P. Xu, who works at Ames Laboratory and Iowa State University, Ames, IA, USA, for communication on the GAMESS calculation; Z.Y.S. also thanks Dr. S. F. Zhang for help in experiments and helpful discussion on the kinematics of reaction microscope.

[1] N. Stolterfoht, Phys. Rev. A **47**, R763 (1993).

[2] R. Schuch, D. Schneider, D. A. Knapp, D. DeWitt, J. McDonald, M. H. Chen, M. W. Clark, and R. E. Marrs, Phys. Rev. Lett. **70**, 1073 (1993).

[3] N. Stolterfoht, C. C. Havener, R. A. Phaneuf, J. K. Swenson, S. M. Shafroth, and F. W. Meyer, Phys. Rev. Lett. **57**, 74 (1986).

[4] A. Hasan, B. Tooke, M. Zapukhlyak, T. Kirchner, and M. Schulz, Phys. Rev. A **74**, 032703 (2006).

[5] M. Zapukhlyak, T. Kirchner, A. Hasan, B. Tooke, and M. Schulz, Phys. Rev. A **77**, 012720 (2008).

[6] A. L. Harris, J. L. Peacher, D. H. Madison, and J. Colgan, Phys. Rev. A **80**, 062707 (2009).

[7] U. Chowdhury, A. L. Harris, J. L. Peacher, and D. H. Madison, J. Phys. B **45**, 035203 (2012).

[8] M. S. Schöffler, J. N. Titze, L. P. H. Schmidt, T. Jahnke, O. Jagutzki, H. Schmidt-Böcking, and R. Dörner, Phys. Rev. A **80**, 042702 (2009).

[9] M. Schulz, T. Vajnai, and J. A. Brand, Phys. Rev. A **75**, 022717 (2007).

[10] H. Andersson, G. Astner, and H. Cederquist, J. Phys. B: At., Mol., Opt. Phys. **21**, L187 (1988).

[11] A. Niehaus, J. Phys. B **19**, 2925 (1986).

[12] H. Cederquist, Phys. Rev. A **43**, 2306 (1991).

[13] A. A. Hasan, E. D. Emmons, G. Hinojosa, and R. Ali, Phys. Rev. Lett. **83**, 4522 (1999).

[14] P. Roncin, M. N. Gaboriaud, M. Barat, A. Bordenavemontesquieu, P. Morettocapelle, M. Benhenni, H. Bachau, and C. Harel, J. Phys. B: At., Mol., Opt. Phys. **26**, 4181 (1993).

[15] P. Roncin, M. N. Gaboriaud, H. Laurent, and M. Barat, J. Phys. B: At., Mol., Opt. Phys. **19**, L691 (1986).

[16] W. Fritsch, Phys. Lett. A **192**, 369 (1994).

[17] W. Lichten, Phys. Rev. **131**, 229 (1963); **139**, A27 (1965); **164**, 131 (1967).

[18] G. N. Ogurtsov, S. Y. Ovchinnikov, J. H. Macek, and V. M. Mikoushkin, Phys. Rev. A **84**, 032706 (2011).

[19] J. Ullrich, R. Moshammer, A. Dorn, R. Dörner, L. Ph. H. Schmidt, and H. Schmidt-Bocking, Rep. Prog. Phys. **66**, 1463 (2003).

[20] D. Fischer, B. Feuerstein, R. D. DuBois, R. Moshammer, J. R. Crespo López-Urrutia, I. Draganic, H. Lörch, A. N. Perumal, and J. Ullrich, J. Phys. B **35**, 1369 (2002).

[21] Y. Xue, R. Ginzel, A. Krauß, S. Bernitt, M. Schöffler, K. U. Kühnel, J. R. C. López-Urrutia, R. Moshammer, X. Cai, J. Ullrich, and D. Fischer, Phys. Rev. A **90**, 052720 (2014).

[22] W. Groh, A. S. Schlachter, A. Murller, and E. Salzborn, J. Phys. B **15**, L207 (1982).

[23] W. T. Rogers, J. W. Boring, and R. E. Johnson, J. Phys. B **11**, 2319 (1978).

[24] P. Moretto-Capelle, D. Bordenave-Montesquieu, A. Bordenave-Monterquieu, and M. Benhenni, J. Phys. B **31**, L423 (1998).

[25] M. A. Abdallah, W. Wolff, H. E. Wolf, E. Y. Kamber, M. Stockli, and C. L. Cocke, Phys. Rev. A **58**, 2911 (1998).

[26] M. N. Panov, in *Electronic and Atomic Collisions*, edited by N. Oda and K. Takayanagi (North-Holland, Amsterdam, 1980), pp. 437–47.

[27] A. A. Basalaev, G. N. Ogurtsov, and M. N. Panov, Tech. Phys. **63**, 947 (2018).

[28] A. A. Basalaev and M. N. Panov, Tech. Phys. **64**, 306 (2019).

[29] J. E. Bayfield and G. A. Khayrallah, Phys. Rev. A **11**, 920 (1975).

[30] U. Fano and W. Lichten, Phys. Rev. Lett. **14**, 627 (1965).

[31] B. Seredyuk, R. W. McCullough, H. Tawara, H B Gilbody, D. Bodewits, R. Hoekstra, A. G. G. M. Tielens, P. Sobocinski, D. Pesic, R. Hellhammer, B. Sulik, N. Stolterfoht, O. Abu-Haija, and E. Y. Kamber, Phys. Rev. A **71**, 022705 (2005).

[32] O. Abu-Haija, E. Y. Kamber, S. M. Ferguson, and N. Stolterfoht, Phys. Rev. A **72**, 042701 (2005).

[33] Z. Y. Song, Z. H. Yang, G. Q. Xiao, Q. M. Xu, J. Chen, B. Yang, and Z. R. Yang, Eur. Phys. J. D **64**, 197 (2011).

[34] M. W. Schmidt, K. K. Baldridge, J. A. Boatz, S. T. Elbert, M. S. Gordon, J. H. Jensen, S. Koseki, N. Matsunaga, K. A. Nguyen, S. Su, T. L. Windus, M. Dupuis, and J. A. Montgomery, J. Comput. Chem. **14**, 1347 (1993).

[35] R. Olson and A. Salop, Phys. Rev. A **14**, 579 (1976).